EDITORIAL CSIC

Scientia Marina
90 (1) January-March 2026, e119
ISSN-L: 0214-8358 eISSN: 1886-8134
https://doi.org/10.3989/scimar.05627.119

ARTICLE

Reproductive biology of the Chilean eagle ray, *Myliobatis chilensis* (Myliobatiformes: Myliobatidae), disembarked in the port of Salaverry, Peru

Biología reproductiva de la raya águila, *Myliobatis chilensis* (Myliobatiformes: Myliobatidae) desembarcada en el puerto de Salaverry, Perú

Miguel Valderrama-Herrera
Escuela de Biología Pesquera, Universidad Nacional de Trujillo, Jirón San Martín 341, Centro Histórico 13001, Trujillo, Perú
miguelvh0294@gmail.com, https://orcid.org/0000-0003-2555-0415

Zoila Culquichicón
Escuela de Biología Pesquera, Universidad Nacional de Trujillo, Jirón San Martín 341, Centro Histórico 13001, Trujillo, Perú
https://orcid.org/0000-0002-4822-1254

Keny Kanagusuku
Área de Laboratorios de Ciencias Naturales, Universidad Científica del Sur, Carretera Panamericana Sur km 19, Villa El Salvador 15067, Lima, Perú;
Carrera de Biología Marina, Facultad de Ciencias Ambientales, Grupo de Investigación de Comunidades Acuáticas, Universidad Científica del Sur, Lima, Perú
Corresponding author: kkanagusuku@cientifica.edu.pe, https://orcid.org/0000-0002-6896-6552

Abstract: *Myliobatis chilensis*, commonly known as the Chilean eagle ray, is a benthopelagic species found along the Humboldt Current. Peruvian fisheries target it, but little is known about its life history. This study aimed to gather information on the reproductive biology of *M. chilensis* from Salaverry. A total of 160 individuals from monthly landings between October 2017 and November 2018 were analysed, with data collected on sex, disc width (DW), clasper calcification, weight, liver and gonads. Sexual maturity was determined by comparing clasper length and clasper calcification in males and by gonadal structure in females. Eighty male individuals (41–153 cm DW) and 80 female individuals (42–221.6 cm DW) were obtained, yielding a sex ratio of 1F:1M. The average ovarian fertility was 32 oocytes, and the median size at sexual maturity was estimated to be 163 cm DW for females and 122 cm DW for males. Histological samples were processed by inclusion in paraplast and stained with haematoxylin and eosin for corroboration. Five stages of ovum development and 11 stages of spermatozoan development were observed. Based on these microstructural observations, a maturity scale with easily distinguishable stages was constructed. The study found that gonads are the sole indicators of maturity in females, while claspers serve as excellent indicators in males. Only mature ovaries were sampled from the second half of each year, and no embryos were found. These reproductive insights are expected to assist in decision-making for sustainable management.

Keywords: Batomorphs; Elasmobranch; Southeastern Pacific; Size at Maturity; Maturity Scale.

Resumen: *Myliobatis chilensis*, comúnmente conocida como raya águila es una especie bentopelágica que se distribuye a lo largo de la corriente de Humboldt. Es objetivo de las pesquerías peruanas; sin embargo, poco se sabe acerca de su historia de vida. El objetivo de este estudio fue recopilar información en su biología reproductiva de *M. chilensis* en Salaverry. Se analizaron un total de 160 individuos de las descargas mensuales entre octubre 2017 y noviembre de 2018, se colectaron datos de sexo, ancho de disco (DW), calcificación de clasper (CC), peso del individuo, de hígado y gónadas. La madurez sexual se determinó comparando el largo de clasper y CC en machos y por estructuras gonadales en hembras. Se obtuvieron 80 individuos machos. (41–153 cm DW) y 80 individuos hembras (42–221.6 cm DW) teniendo una proporción de 1F:1M. La fertilidad ovárica promedio fue de 32 oocitos, y la talla media de madurez sexual (MSM) fue estimada en 163 cm DW para hembras y 122 cm DW para machos. Las muestras histológicas fueron procesadas por inclusión en paraplast y teñidos con and hematoxilina-eosina para la corroboración. Se observaron cinco estadios de desarrollo ovárico y once para desarrollo espermático. Basado en las observaciones de estas microestructuras, se construyó una escala con estadios fácilmente distinguibles. El estudio halló que las gónadas son los únicos indicadores de madurez en hembras, en tanto, los claspers sirven como excelentes indicadores en los machos. Únicamente se muestrearon ovarios maduros en la segunda mitad del año y no se han encontrado embriones. Se espera que estos hallazgos acerca de la reproducción puedan asistir a en la toma de decisiones para el manejo sostenible de la especie.

Palabras clave: batoideos; elasmobranquios; Pacífico sudeste; talla de madurez; escala de madurez.

Editor: P. Brosset

Received: 27-02-2025 / **Accepted**: 04-10-2025 / **Published**: 22-06-2026

Citation: Valderrama-Herrera M., Culquichicón Z., Kanagusuku K. 2026. Reproductive biology of the Chilean eagle ray, *Myliobatis chilensis* (Myliobatiformes: Myliobatidae), disembarked in the port of Salaverry, Peru. Sci. Mar. 90(1): e119. https://doi.org/10.3989/scimar.05627.119

Supplementary information ↓

1. INTRODUCTION

Myliobatis chilensis Philippi, 1892, commonly known as the Chilean eagle ray (Chirichigno and Vélez 2008), is one of the most important species of Chondrichthyes for Peruvian fisheries. Off the northern coast of Peru, eagle rays of the genus *Myliobatis* are targeted (PRODUCE 2018, Veneros Urbina and Amaya Alvarado 2021), with catches primarily (though not exclusively) occurring when more profitable species are scarce. Batomorphs are also a part of the local gastronomy: inhabitants of the regions of La Libertad and Lambayeque have been the main consumers of batomorphs since pre-Columbian times (Bradley 2012). However, information about the species remains limited.

M. chilensis has a distribution along the temperate waters of the Humboldt Current (Chile–Peru) (Zavalaga *et al.* 2021) and can reach up to 254 cm in disc width (DW) (González-Pestana *et al.* 2020). It exhibits pelagic habits and is found on the continental shelf (Zavalaga *et al.* 2021); it can also reach the benthos to feed, though it does not settle there. The maximum depth it reaches or frequents remains unclear, as do its population size and individual longevity. Furthermore, critical data regarding its size at sexual maturity, size at birth, age at sexual maturity, gestation period, reproductive cycle and population growth rate remain unknown (Dulvy *et al.* 2020).

Although the Chilean eagle ray is commonly fished today, its potentially low fecundity, along with limited of knowledge of its reproductive and gestation periods, could reduce its availability in the future. The species is currently classified as vulnerable by the International Union for Conservation of Nature (Dulvy *et al.* 2020). As a predator (González-Pestana *et al.* 2020), its disappearance could destabilize the community

dynamics of the local marine ecosystem. Furthermore, its population would likely take years to recover due to its possible low reproductive output. Therefore, studies on the reproduction of this species are crucial for achieving optimal fisheries management and ensuring the sustainable use of the species.

2. MATERIALS AND METHODS

The research was conducted at the port of Salaverry (8°13'42.35" S; 078°58'50" W), located 14 km southeast of Trujillo in the La Libertad region, an area with significant artisanal fishery activity (Fig. 1). Sampling took place from October 2017 to November 2018, with landed individuals from local artisanal fisheries at the pier.

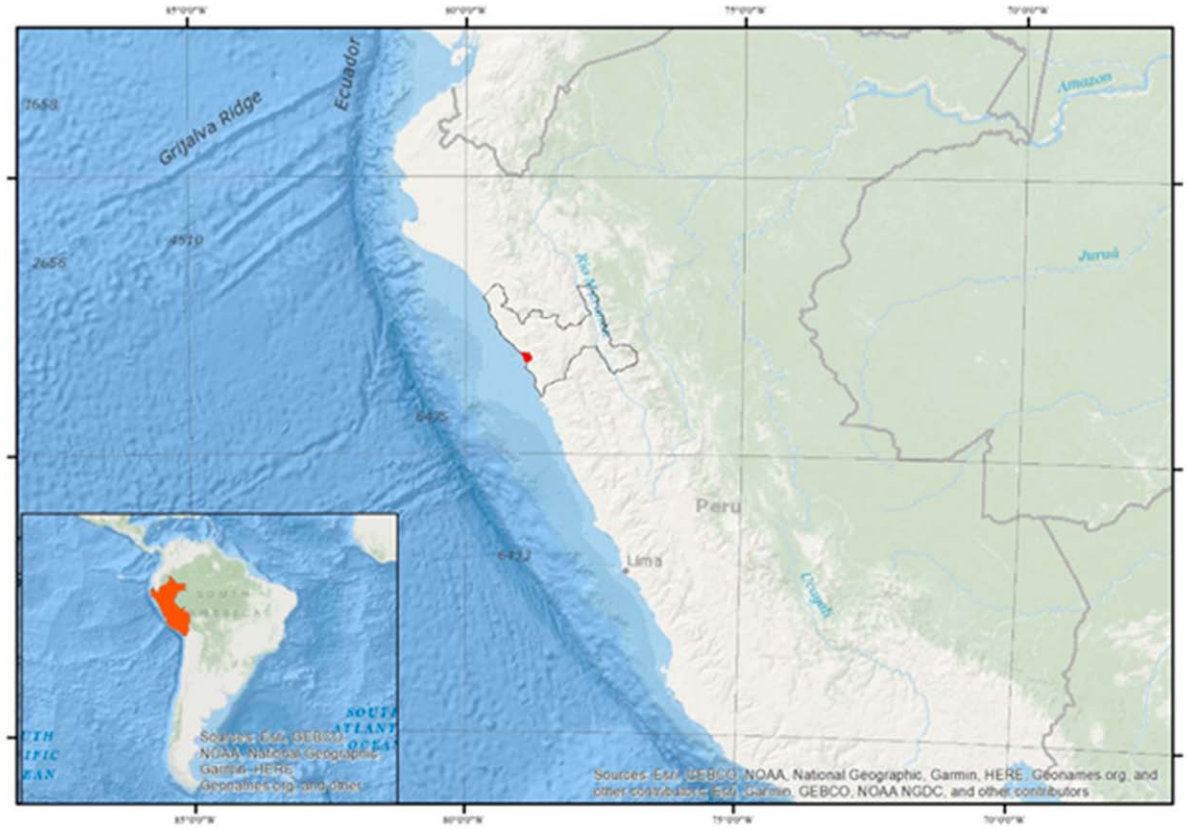

Figure 1. Location of Salaverry port in La Libertad, along the northern Peruvian coast.

Rays were typically captured using locally known fishing nets called *redes rayeras* (ray nets), which are 80 to 100 fathoms long and have a mesh size of 14 to 15 inches. These nets are set in the water column (approximately 10 m deep) or near the surface. Occasionally, snook nets, or *redes robaleras* (bass nets), with an 8-inch mesh size and 50 fathoms in length, were also used. Since two *Myliobatis* species (*M. chilensis* and *M. peruvianus*) are present in the area, the dental plate of each individual was examined to distinguish between them. In *M. chilensis*, the dental plate features 8 to 12 vertical rows on the upper jaw, with central teeth slightly larger than the lateral ones. In contrast, *M. peruvianus* has seven dental rows, with the central teeth in the upper jaw markedly larger than those on the three lateral rows (Sáez and Lamilla 2012, Zavalaga *et al.* 2021). All individuals examined in this study were landed at the pier and were already dead upon inspection, so ethical review and approval were not required for this animal study.

Individuals were randomly selected from the total catch. The following data were recorded: DW, total weight (W), and, for males, clasper length (CL) and calcification. A ventral incision was then made, extending from the pectoral girdle to the anus, to extract the liver and gonads. The samples were transported to the Laboratory of Aquatic Resources at the School of Fisheries Biology, Universidad Nacional de Trujillo, where the liver and gonadal weights were measured, along with gonad length

and width. Gonad samples were preserved in 4% neutral formalin, ensuring complete coverage of the structures for later histological preparation, which involved embedding in Histosec and staining with haematoxylin and eosin (Tresierra *et al.* 2002, Nureña 2018, Ganias *et al.* 2025).

The prepared slides were taken to the Peruvian Marine Institute (IMARPE) in Chimbote, Ancash, for examination under a Leica ICC50 HD compound microscope. Micrographs were captured using Leica Application Suite Version 45.0 software. For macroscopic determination of maturity stages, the scale of Holden and Raitt (1975), as cited by Tresierra *et al.* (2014), Tresierra and Culquichicón (1993), Acevedo *et al.* (2007), Colonello *et al.* (2007), and Grijalba-Bendeck *et al.* (2012), was used as a reference (available in Supplementary material).

Fecundity was assessed by counting the vascularized oocytes, as they have the highest probability of being fertilized. The diameter of the oocytes was also measured. Size composition and sex ratio were calculated using the formula outlined by Wenner (1972), as cited by Tresierra *et al.* (2014).

$$\%\text{males or females} = \frac{\text{Nm}}{\text{Nt}} * 100$$

where *Nm* is the number of males or females and *Nt* is the total number of individuals.

A χ^2 test was applied with a 95% confidence interval, the null hypothesis being the expected ratio of 1:1 (H_0).

$$X^2 = \sum \frac{(O-E)^2}{E}$$

where 0 is the observed value and E the expected value.

Diagrams of general and monthly proportions of the maturity stages in females and males were produced (Grijalba-Bendeck *et al.* 2012). To corroborate maturity (Vélez 2015), scatter plots were constructed for evaluation using linear regression, comparing DW and W, DW and CL, DW and gonad length, and DW and number of oocytes.

Biological indexes were used to infer gonadal maturation phases: gonadosomatic index (GSI) (Tresierra *et al.* 2014) and hepatosomatic index (HI) (Tresierra *et al.* 2013):

$$\text{GSI} = \frac{W_G}{W_B} * 100$$

where W_G is the gonad weight and W_B is the body weight;

$$\text{HI} = \frac{W_H}{W_B} * 100$$

where W_H is the liver weight and W_B is the body weight.

The mean size at gonadal maturity, or simply the mean size at maturity, was estimated with the formula:

$$P = \frac{1}{1+e^{a+b \cdot L}}$$

where *P* is the probability of maturity, *a* and *b* are model parameters and *L*is the length (DW).

The logistic model was used to estimate the size at which specimens reach sexual maturity, as it identifies the DW at which 50% of individuals are capable of reproduction.

Correlations between structures were evaluated using the coefficient of determination (R^2) obtained from the equations describing the data trends.

3. RESULTS

A total of 160 individuals were sampled over the course of one year, excluding January and February, when no landings occurred.

3.1. Size conformation

A predominance of smaller sizes was observed, with the majority of individuals falling within the 40–90 cm DW range. The smallest female measured 42 cm DW, while the smallest male measured 41 cm DW. The largest female measured 221.6 cm DW (Fig. S1; Supplementary material), while the largest male measured 150 cm DW. The average DW was 93.63 cm for females and 84.63 cm for males. The medians and means were very similar in both sexes: 75.75 cm (median) and 61 cm (mean) for females, and 75.5 cm (median) and 60 cm (mean) for males (Table 1) (Fig. 2).

Table 1. – Report of sampled specimens per month, October 2017–November 2018. AS (DW), Average size (disc width); SD, standard deviation.

Month	♂	♀	Total	AS (DW) ♂	SD ♂	AS (DW) ♀	SD ♀
October	2	4	6	63.5	4.19	57	4.42
November	9	5	14	48.41	31.13	48.38	31.14
December	4	7	11	79.5	60.27	154.14	59.21
January	0	0	0				
February	0	0	0				
March	8	7	15	75.5	16.13	65.93	16.14
April	2	5	7	106.00	31.99	108.4	31.98
May	5	7	12	65.86	7.73	62.01	7.72
June	2	5	7	68	9.06	69.3	9.06
July	3	4	7	63.27	6.26	57.825	6.22
August	17	11	28	103.53	44.00	140.05	44.29
September	7	8	15	67	40.06	100.75	40.01
October	7	7	14	84.51	12.47	78.17	12.47
November	14	10	24	79.63	15.51	77.45	15.52
Total	80	80	160	84.64	36.66	93.47	36.66

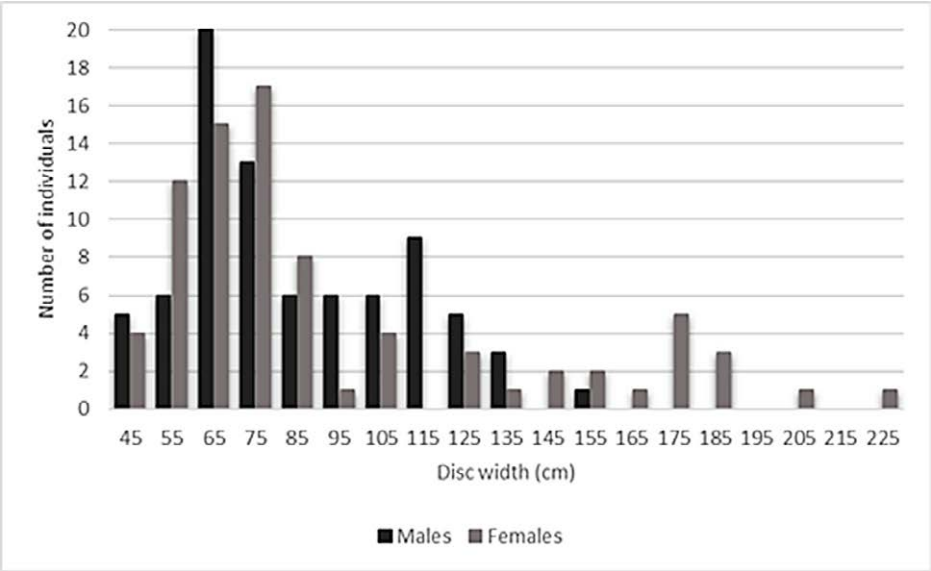

Figure 2. Total composition of sampled individuals' sizes.

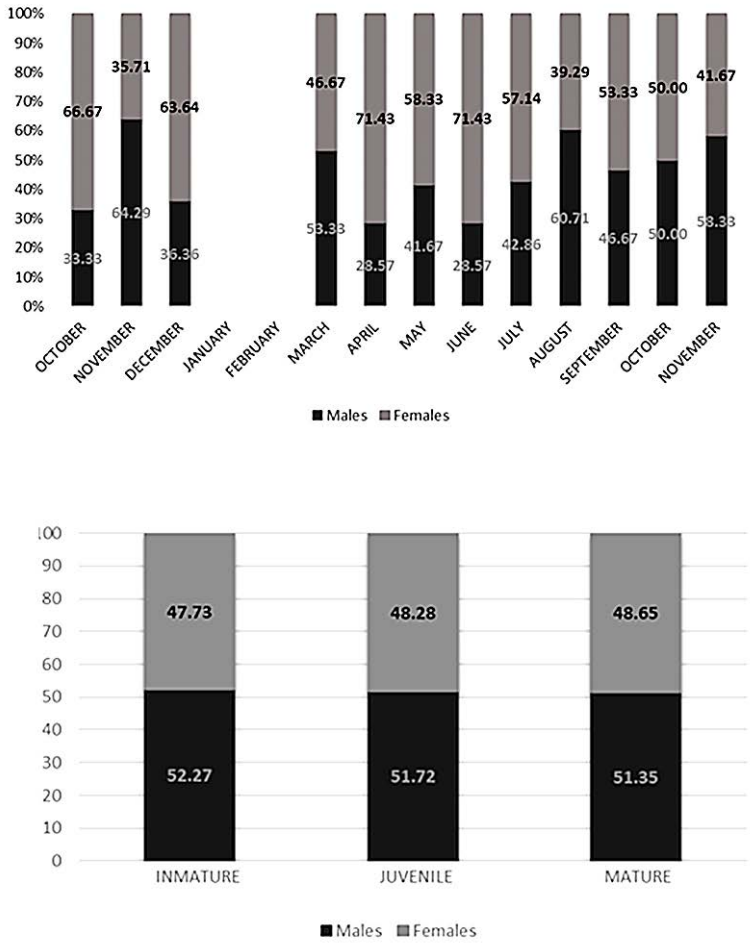

Figure 3. Sex ratio in *M. chilensis*, per month (a) and by maturity stage (b). The pattern is quadratic (c), showing a dominance of males between 90 and 130 cm DW that then decreases. This was evaluated only in males, so the percentage in females is opposite.

3.2. Sex ratio

The overall sex ratio was evenly balanced, with 80 females and 80 males, equivalent to 1F:1M. Monthly variation was observed (Fig. 3A), with a higher proportion of females recorded in April and June (71.43% in both months). It is worth noting that during these months, the number of landings decreased significantly, and in June, only immature individuals were observed. Males predominated in November 2017 and 2018, representing 64.29% and 58.33% of individuals, respectively.

Across maturity stages, the sex ratio also remained at 1:1 (F:M), with no statistically significant difference (χ^2=0.243; p>0.05) (Fig. 3B), although a slight male predominance was noted. Regarding sex ratio by size class, the pattern followed a quadratic distribution (Fig. 3C), with male dominance observed between 90 and 130 cm DW, followed by a decline from 150 cm DW onwards due to their absence.

3.3. Weight–length ratio

This ratio exhibited a quadratic pattern (Fig. 4, top), in which the exponent (b) was 3.04 for females and 3.09 for males, indicating isometric growth for both sexes. Ultimately, both models were linearized (Fig. 6, bottom).

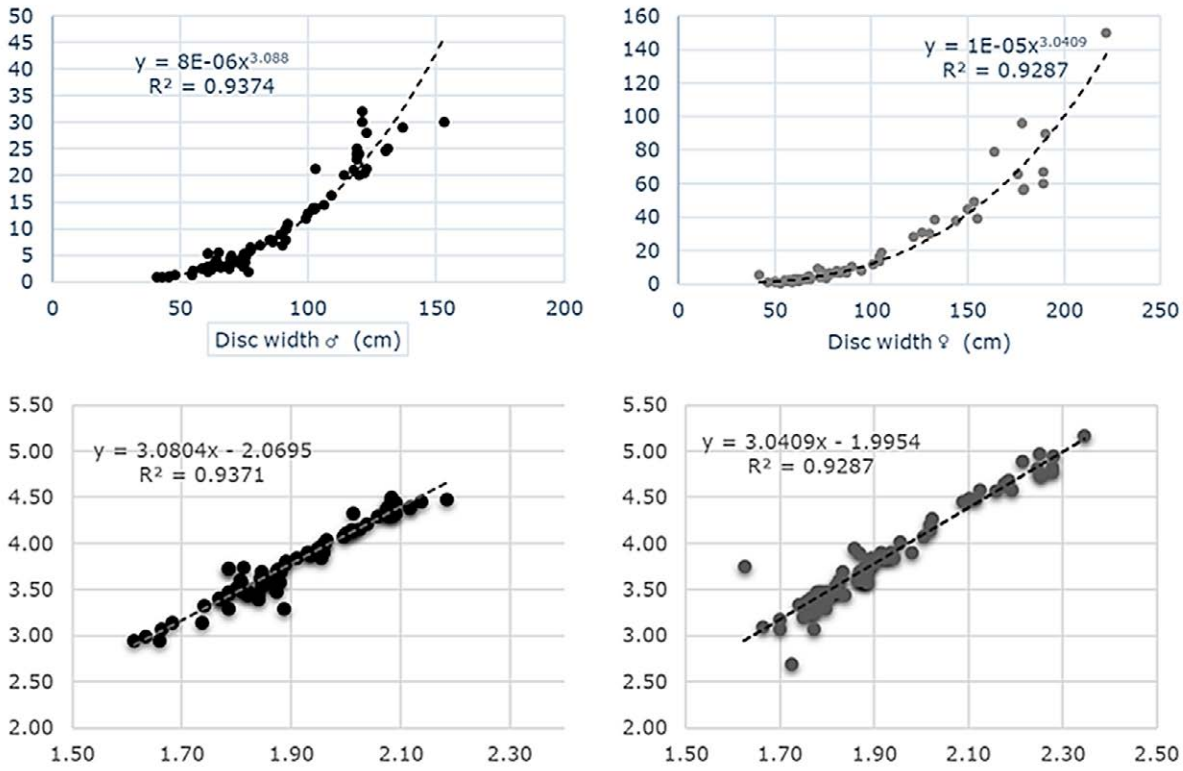

Figure 4. – Weight–length ratio in *M. chilensis*, males (left) and females (right) potential (top) and linearized (bottom).

3.4. Gonadosomatic index

The index was assessed in 111 individuals (Fig. 5). The highest GSI values in females were recorded in December 2017. During this period, males also showed an increase in GSI, although their values did not reach a peak or match those observed in females. The highest GSI values for males occurred in July; however, all individuals sampled during this month were immature. Between October and November 2018, both sexes exhibited similar GSI values.

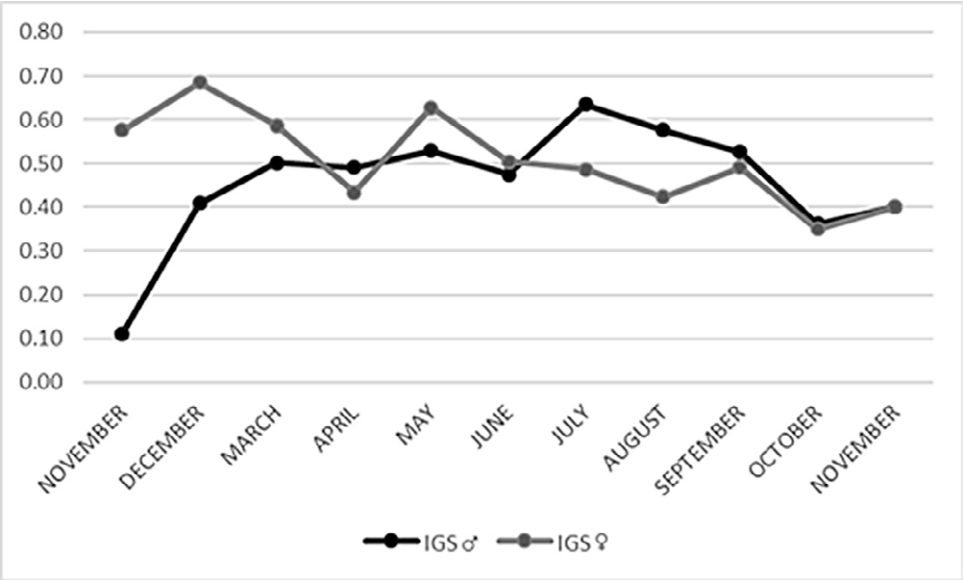

Figure 5. Validation in gonadosomatic index (GSI) per month of *M. chilensis*.

3.5. Hepatosomatic index

The ratio of liver weight to body weight was assessed in 156 individuals (Fig. 6). In October 2017, HI values were similar between sexes. Thereafter, values remained relatively stable in females but declined in males. An increase was observed in both sexes during December 2017 and March 2018. Towards the end of the austral summer and the beginning of winter, HI values became more variable and interspersed between sexes. At the onset of winter, HI values declined in both sexes before rising again in August. A crossover in trends reappeared in September and levelled off in October, ending in November with both sexes showing similar values once more.

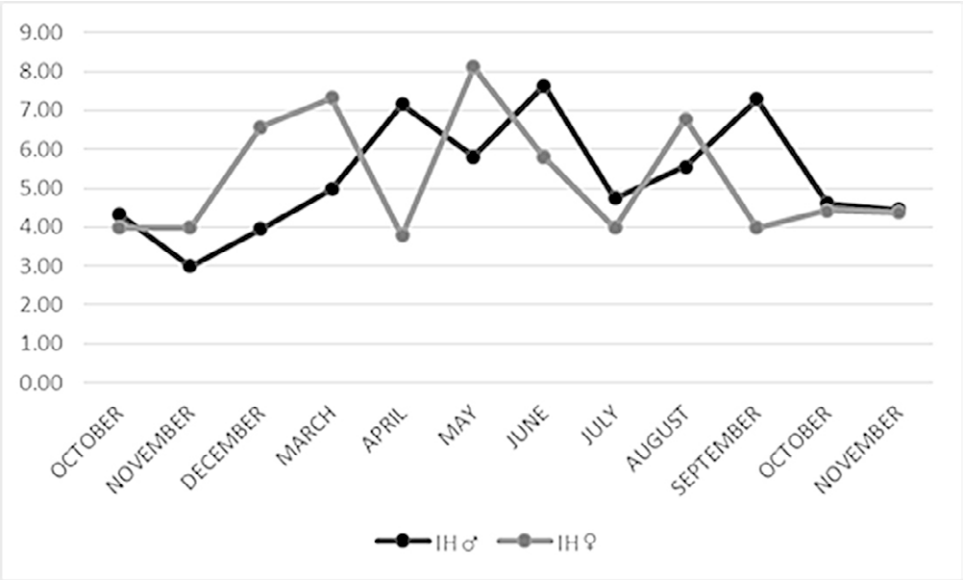

Figure 6. Variation in hepatosomatic index (HI) per month of *M. chilensis*.

3.6. Stages for females

Female maturity was categorized into five stages, as presented in Table 2. However, the final stages (gravid females and postpartum) were not observed in the sampled individuals.

Table 2. – Female gonadal development scale for *Myliobatis chilensis*. Two extra stages proposed: pregnant and post-partum; however, they were not found during this study.

Stage I: Immature	Gonads An immature ovary is characterized by having an abundant epigonal organ and being fragile, whitish in colour; the haematopoietic organ that surrounds it is dark red. Oviducts are indistinguishable. Differences between left and right ovary's sizes are minimum.	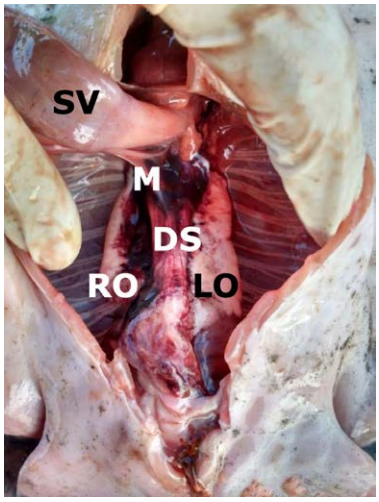 SV, spiral valve; DS, dorsal spine; M, mesovarium; LO, left ovary; RO, right ovary.
Stage II: Pre-mature or juvenile	Gonads: Ovaries increase in size, their colour varies from whitish to orange and there is already greater development of the left ovary. Previtellogenic oocytes are barely differentiated. Oviducts can be visualized as well as the formation of what will be the uterus. The juvenile ovaries in the final phases show some small vitellogenic oocytes visible to the naked eye and not irrigated.	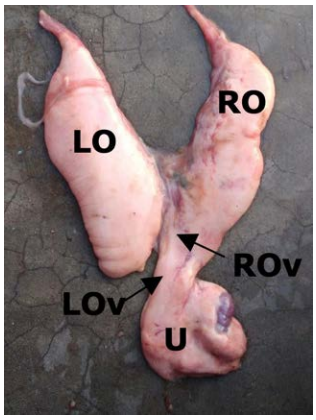 ROv, right oviduct; LOv, left oviduct; U, uterus; LO, left ovary; RO, right ovary.
Stage III: Mature non-pregnant	Gonads: Epigonal organ completely covers the remnant of the right ovary, which is nothing more than a reduced compact structure. By contrast, the left ovary is noticeably large (reaching 26 cm in length and 8 cm in width), translucid in colour and has an almond-like shape. Oocytes are distinguishable to the naked eye, being yellowish-orange and highly vascularized. Uterus: Uteri are evident and have a cylindrical-oval shape and many tissue layers, making them hard to touch. Their highly vascularized interior contains trophonemata—dark red villi specialized in nourishing the developing embryos.	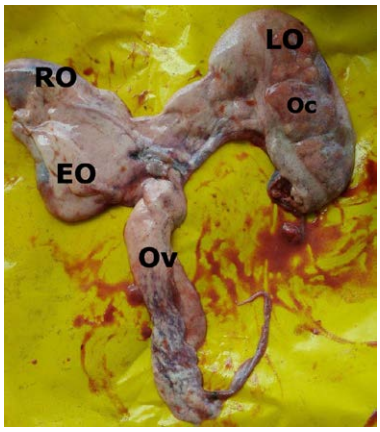 EO, epigonal organ; Ov, oviduct; LO, left ovary; RO, right ovary; Oc, oocytes.

Immature. A total of 42 immature females were collected, with DW ranging from 42 to 87 cm (mean±SD: 69.75±12.55 cm). Ovaries were whitish and fragile in appearance (n=33), measuring between 7 and 15 cm in length (9.42±1.96 cm). The uteri were poorly developed and barely distinguishable from the oviducts.
Juvenile or pre-mature. Juvenile females (n=14) ranging between 63 and 126 cm DW (87.39±18.57) were recorded. Ovaries gained size, being between 9 to 19 cm in length (12.28±3.05), Ovaries had increased in size (9–19 cm; 12.28±3.05 cm) and varied in colour from whitish to orange. Uteri began to differentiate and were more easily identified.

Mature. The smallest mature female measured 122 cm DW, while the largest measured 221.6 cm DW (173.63±23.32 cm). A total of 18 mature females were collected. The right ovary was consistently smaller than the left, the latter being the only side producing oocytes. Left ovaries measured between 12 and 26 cm (18.73±4.60 cm) in length and 3 and 8 cm in width (6.15±1.46 cm). Eight well-preserved uteri were collected, with lengths ranging from 13 to 38 cm (20.13±8.10 cm) on the left and 13 to 26 cm (16.31±4.25 cm) on the right.

3.7. Disc width–ovary length ratio

A total of 55 females were analysed to assess the relationship between DW and the length of the left ovary (LO), the only functional ovary in this species. The data showed overlapping ranges across stages, with a stage transition between 76 and 79 cm DW. Juvenile individuals were the least represented, with only 9 sampled. The final maturity transition occurred at 130 cm DW, corresponding to the smallest mature female recorded. A strong linear correlation was found between DW and LO (R=0.9039, R^2=0.8171) (Fig. 7).

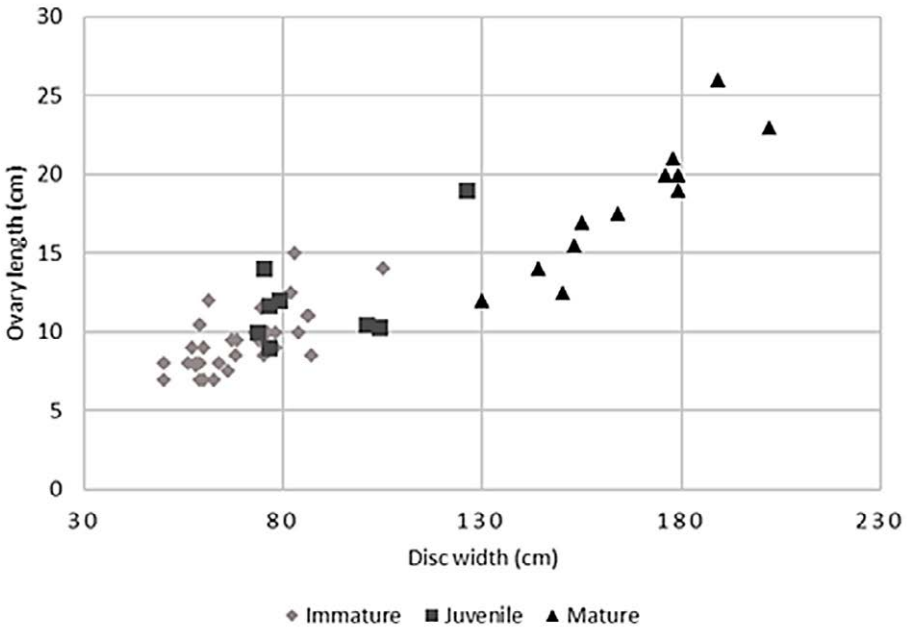

Figure 7. Relation between disc width and left ovary length.

3.8. Disc width, number and oocyte diameter ratio

This analysis was conducted on 10 individuals (Fig. S2), considering only vitellogenic oocytes. On average, 32 oocytes were recorded per individual. The smallest female with vitellogenic oocytes measured 150 cm DW and had 26 oocytes, while the largest measured 202 cm DW and had 35 oocytes. The oocytes reached substantial sizes, with the largest measuring 42 mm, nearly the minimum diameter of a standard golf ball (Table 3). A potential positive relationship was found between specimen size and both the number of developed oocytes (r=0.5049) and ovary size (r=0.53). However, no correlation was observed between DW and average oocyte diameter (r=0.0245).

Table 3. – Percentage of oocytes over the average diameter. Disc width (DW), left ovary length (LO), oocyte number (N), percentage (%) and diameter of the biggest oocyte (BO) are specified.

DW	LO	N	%	BO
179	20	16	52	26.19
189	26	27	55	34.5
189	26	10	27	42
202	23	17	49	29
179	19	12	57	33
150	12.5	15	58	29
144	14	5	38	23
155	16	32	67	28
176	18	22	76	35
164	17.5	13	93	30

Female reproductive system. The female reproductive system can be divided into four main components: ovaries, ducts, uterus and cloaca.

In vertebrates, reproductive structures are generally paired; however, in *M. chilensis*, those on the left side show greater development. The right ovary is reduced in size and becomes non-functional for ovum production. Another notable feature is the absence of an oviducal or nidamental gland.

Both ovaries are located in the anterior-dorsal region of the body, supported by the mesovarium (mesovarian folds), and are covered by the epigonal organ. The epigonal organ varies in prominence, being more abundant in the right ovary and in immature specimens.

The ovarian follicles are soft to the touch and delicate. Follicles at various developmental stages are present within the parenchyma, with the most advanced ones located near the cortex (also known as ovarian wall). Oocyte colour is an indicator of developmental stage: immature oocytes appear translucent-whitish, while vitellogenic oocytes are yellowish. Oocyte size is substantial, with the largest recorded at 42 mm in diameter. Mature oocytes exhibit abundant vascularization and are surrounded by multiple cell layers (granulosa zone).

The oviducts continue to the uterus (Fig. S3), a bifurcated structure with greater development on the left side. Macroscopic distinction is not possible in immature individuals, given the impossibility of determining where the oviducts end and the uteri begin. As they mature, the uterine walls develop several layers of tissue, widen and become rigid, adopting a cylindrical shape that gradually becomes oval, making the structure evident. The uterine interior is highly vascularized, and trophonemata (flat, thin, reddish villi) develop within. These are specialized structures in myliobatids for embryonic nourishment through the production of a whitish, translucent secretion known as histotrophy or “uterine milk”. Ultimately, both uterine branches lead to the cloaca, through which pups are expelled.

Microstructure. In immature ovaries (Fig. S4B), the epigonal organ almost entirely envelops the structure, and no oocytes were observed in the earliest maturity stage. The tunica albuginea was also absent. The epigonal organ resembles the human thymus, composed of clusters of red blood cells within pseudolobes lacking defined borders or continuous connective tissue (Fig. S4A). Dense connective tissue was present where the ovarian capsule begins to form.

In juvenile ovaries (Fig. S4C, D), the epigonal organ remained present across much of the tissue, although the ovarian edge showed increased connective tissue, apparently representing the germinal zone, as oocytes at the vitellogenic stage were observed developing here (Fig. S4C). At this stage, the oocytes have developed the zona granulosa, but the ovarian follicle is not ready to ovulate. The right ovary still contains epigonal tissue and dense peripheral connective tissue, but no oocyte development was observed (Fig. S4D). Internally, collagen fibres begin to form, likely providing the rigidity required for subsequent structural development.

In mature ovaries, the epigonal organ is limited to the ovarian edges and the region adjoining the mesovarium. Ovarian walls are enlarged and contain abundant collagen fibres, followed by fibroblasts and, finally, cuboidal epithelial cells. The false albuginea, located beneath the epithelium, is made up of dense connective tissue rich in collagen and elastin. The interior comprises a cortex made of parenchyma (cells capable of dividing) and stroma (non-dividing supportive tissue). Oocytes within the cortex are considerably large, making histological sectioning difficult (Fig. 5B). Maturing oocytes are found near the cortical edge, where cuboidal cells will later form the surrounding follicular cells. Several large oocytes were found grouped alongside smaller ones, possibly fusing into a larger structure.

In the right ovary, no developed oocytes were observed. Only peripheral fibroblasts, stroma and lobules with acini lined by epithelium were observed. Gonadal development in females was classified into five stages, as presented in Table 4 and Figures S5-S7 of the Supplementary material. In mature females, trophonemata were observed, these structures sprouted from the myometrium, were vascularized, and contained secretory cells (Figs S9-S10).

Table 4. Oocyte development scale of *M. chilensis*.

Oocyte stage	Characteristics
Stage I	An obvious reduced size. Surrounded by flat cells and with a nucleus near the cell edge.
Stage II	The zona pellucida is observed with simple cuboidal epithelium and connective tissue. Nucleus with visible nucleoli.
Stage III	Pre-vitellogenic oocytes, the nucleus does not undergo major changes, but the nucleoli are no longer perceptible. The zona pellucida increased in size with the multiplication of cubic cells. Part of these will give rise to the columnar epithelium, made up of cylindrical cells. Fibroblasts and collagen fibres are found in the periphery.
Stage IV	The oocyte is increased in size and yolk granules are observed in the cytoplasm. The cell layers are thickened and now the zona pellucida or radiata, zona granulosa or corona radiata, theca interna and theca externa can be distinguished. Each layer is distinguished by the type of cells that make it up: the zona radiata, composed of glycoproteins, is quite acidophilic and can therefore be stained with eosin; the granulosa is composed of the columnar epithelium, cylindrical cells with basophilic nuclei at their base. The basement membrane, a continuous protein sheet, and the presence of some blood cells are observed; the internal theca is composed of loose connective tissue, acidophilic collagen fibres and, finally, the external theca with cubic cells.
Stage V	The follicular structure is basically the same as in the previous stage, but the size varies enormously: a vitellogenated oocyte in stage IV can measure 400–500 μm, while one in stage V reaches 30–40 mm. To achieve such massive dimensions, the oocyte tends to fuse with others. The cell layers must ensure continuous nutrition for such a large cell, so they increase in thickness. The theca externa is now quite vascularized and even the granulosa tends to form folds and develop goblet cells that secrete mucoproteins.

3.9. Stages for males

Three gonadal maturity stages were identified in males (Table 5). Unlike in females, all stages were represented among the sampled individuals.

Table 5. Male gonadal development scale for *M. chilensis*. C, clasper; T, tail; PF, pelvic fin; EO, epigonal organ; V, sperm vesicle; LT, left testis; RT, right testis; ED, efferent duct

	Claspers		Gonads	
Stage I: Immature	Small, not longer than 6 cm, they do not extend beyond the posterior edge of the pelvic fin and are evidently flaccid.	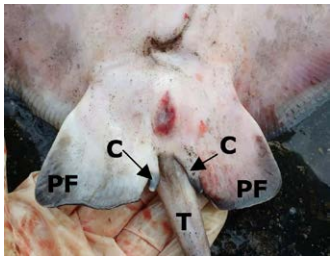	The testicular structure is watery, fragile and whitish in colour. A few poorly developed sperm vesicles can be observed, but most of the structure is covered by the epigonal organ. The ducts are barely distinguishable and no epididymis or seminal vesicle is observed.	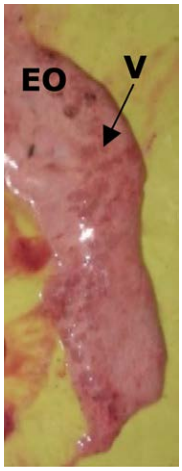
Stage II: Pre-mature or juvenile	There is an increase in size, reaching beyond the pelvic fins. To the touch, there is greater rigidity, but they are not yet completely calcified. Rhipidion closed.	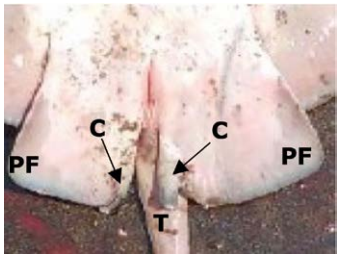	Increase in size of the testes, and sperm vesicles are now clearly visible. They adopt a depressed shape and a pinkish colour while the cream-whitish colour is restricted to the epigonal organ.	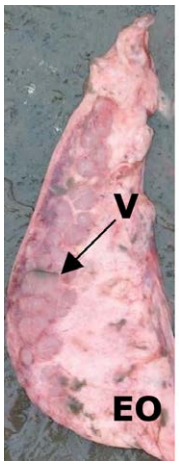
Stage III: Mature	Measured from their base, they reach 17 cm, although most of those collected measured 15 cm. They are completely calcified, and it is possible to rotate them at an angle of 360°. The distance that separates the tip of the claspers from the edge of the pelvic fins is evident. The rhipidion is open.	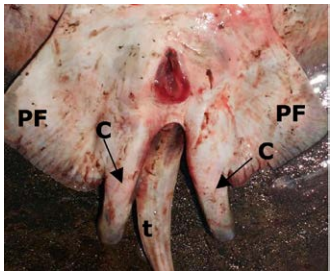	Prominent sperm vesicles are easily distinguishable and, combined with the dorsoventrally depressed shape, gives the appearance of a bunch of grapes. The epigonal organ is greatly reduced and restricted to the testicular periphery. The epididymides are firmly attached to the edge of the spine, and the ducts and seminal vesicle are easily distinguishable.	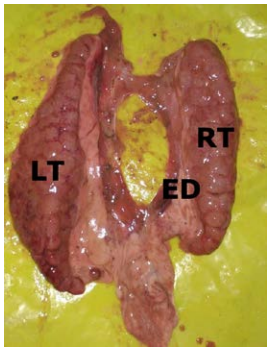

Immature. Immature males were the most abundant, with 46 individuals between 41 and 89 cm DW (65.73±10.99 cm). Claspers were barely distinguishable, ranging from 3 cm to 7 cm in length. Testes were watery and whitish in appearance, with lengths ranging from 4.5 to 14.2 cm for the left (9.71±2.29) and 3.2 to 12.5 cm for the right (7.26±1.80): Spermatic ducts and vesicles were poorly developed and difficult to distinguish.

Juvenile. The DW of juveniles (n=15) ranged between 72 and 109 cm (94.41±10 cm). Claspers increased in size, measuring between 7 and 14 cm (9.06±2.04 cm). Regarding the testes, a change to a more pinkish colour and an increase in size were observed: between 8 and 22.2 cm for the left (14.28±4.07) and between 6 and 19 cm for the right (11.33±3.27). At this stage, spermatic ducts and vesicles were clearly differentiated.

Mature. Nineteen mature males were examined, with DWs ranging from 103 to 153 cm (122.72±10.07 cm). Claspers were evidently larger and fully developed, reaching up to 15 cm (14.69±0.63 cm). The testes showed slight asymmetry between left and right, but the overall structure was similar. Right testis lengths ranged from 13 to 19.7 cm (16.64±1.91 cm), while left testis length ranged from 15.5 to 25 cm (19.79±2.81 cm). The testes were pinkish and rich in spermatic vesicles, indicating active reproductive capacity.

3.10. Disc width–clasper length ratio

The CL was recorded for all male individuals (n=80) (Fig. S11). The minimum size was 4 cm, which remained constant for the sizes between 40 and 60 cm DW. Transition was observed at approximately 7 cm CL and DWs between 80 and 90 cm.

Among the juveniles, the sizes of the copulatory organ ranged from 7 to 14 cm. They were in the calcification stage, with some already showing considerable rigidity, although the rhipidion remained closed. In contrast, mature claspers were significantly larger and thicker, with open rhipidion and the ability to rotate, features indicative of full sexual maturity. The final transition occurred at 14 cm CL and 114 cm DW, with all individuals at or beyond these measurements being sexually mature. A strong linear correlation was found between DW and CL (r=0.9320).

3.11. Male reproductive system

The basic structure of the male reproductive system is made up of five parts: testes, epididymis, conducts, seminal vesicle and copulatory organs. The reproductive organs are paired without significant differences regarding sizes between the left and right side. The testes are of the compound type (Pratt 1988, Engel and Callard 2005, Conrath and Musick 2012), appearing as elongated, flattened structures resembling a laterally compressed bunch of grapes. They are suspended by the mesorchium and are light pink in colour. In contrast to females, the asymmetry between the left and right testis is minimal, although, as with the ovaries, the left testis tends to be slightly larger.

The efferent ducts connect the testes to the epididymis, a light pink to orange structure averaging 15 cm in length, located near the spinal column. The vasa deferentia continue from the epididymis to the seminal vesicles, where sperm is stored prior to ejaculation through the claspers.

Claspers are specialized copulatory organs formed by extensions of the pelvic fins. When mature, they reach up to 15 cm in length and are fully calcified and permanently rigid. During sexual intercourse, one clasper is inserted into the female's cloaca, allowing internal fertilization through ejaculation. At the anterior base of each clasper and near the junction with the pelvic fin, there is an opening called the apopyle. At the posterior tip is another, more prominent opening called the hypopyle, which is partially covered by the rhipidion. Complete coverage of the hypopyle by the rhipidion indicates that the individual is not yet reproductively active. As in females, the testes are initially covered by the epigonal organ, which gradually regresses as the individual matures. Both testes are functional, and spermatogenesis occurs in 11 distinct phases, which are detailed in Table 6 and Figures S12- S15 of the Supplementary material.

3.12. Median size at sexual maturity

One of the most significant findings of this study was the determination of the DW at which 50% of individuals were sexually mature. This measurement was determined as 122.22 cm for males and 163.16 cm for females (Fig. 8). The smallest female with vitellogenic oocytes was 144 cm DW. From 160 cm DW onwards, females consistently exhibited an LO longer than 17 cm and approximately 6 cm in width, along with well-developed uteri exceeding 15 cm in length and 5 cm in width.

The smallest male with a developed clasper was 103 cm DW. From 114 cm DW onwards, all males had fully calcified, rotatable claspers with open rhipidion. At 120 cm DW, testes had reached a minimum of 17 cm in length for the left testis, 15 cm for the right, and 4 cm in width, which is indicative of full reproductive capability.

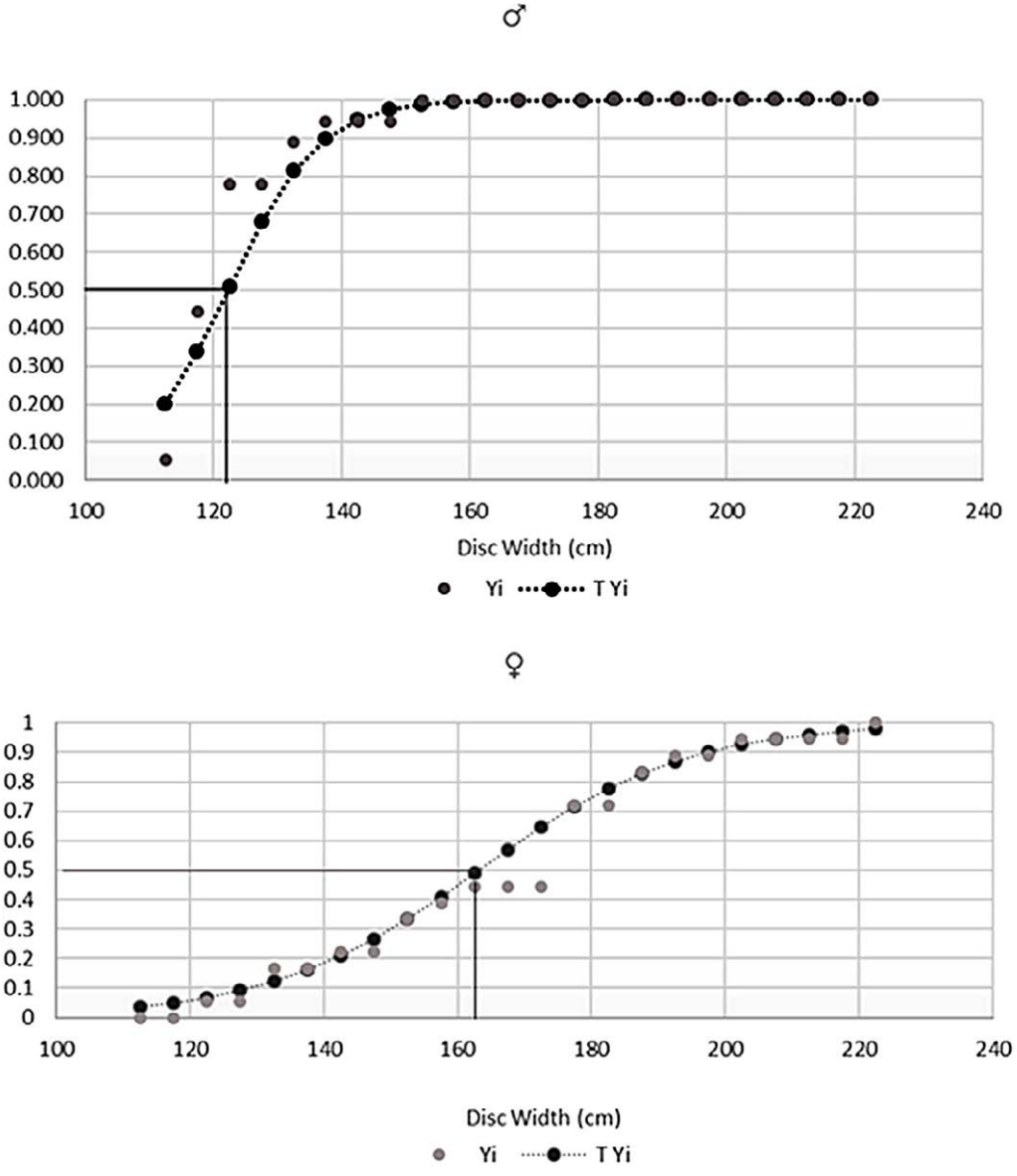

Figure 8. Median size at sexual maturity for males (♂) and females (♀), showing observed values (Yi) and theorical calculated values (T Yi).

Table 6. – Spermatogenesis scale of *M. chilensis*.

Development stage	Characteristics
Phase I	The cysts develop spermatogonia, characterized by a large basophilic nucleus and loose chromatin.
Phase II	Arrangement of the spermatogonia around the cyst, leaving a central lumen. Sertoli cells (whitish in colour) also migrate toward the periphery.
Phase III	Condensation of the chromatin in the spermatogonia and division; they will end up being placed one on top of the other.
Phase IV	Meiotic divisions resulted in spermatocytes I, smaller cells with a nucleus with fairly condensed chromatin. The cyst increases in size.
Phase V	The new divisions give rise to spermatocytes II, smaller cells with condensed nuclei.
Phase VI	Spermatocytes II lengthen and are reduced in size.
Phase VII	The haploid cell, the spermatid, finishes developing.
Phase VIII	Reduction of the head and elongation of the flagella of the spermatids to develop as spermatozoa. The head moves to the cytoplasm of the Sertoli cells and the flagella projects towards the lumen.
Phase IX	The sperm are fully developed and are in a “spiral arrangement”.
Phase X	The sperm compact together to form “packages” that will be expelled through a process called spermiation.
Phase XI	The cysts are now residual follicles with some sperm or Sertoli cells remaining. These cells will be reabsorbed.

4. DISCUSSION

During the period from October 2017 to November 2018, maritime conditions were normal. The exceptional El Niño events experienced during the summer of 2017 had subsided by October of that year (Grupo de Trabajo Institucional El Niño 2017). No anomalous oceanographic conditions were recorded throughout 2018. As a result, the biological and reproductive parameters evaluated in this study can be considered representative of the species under normal environmental conditions.

4.1. Size distribution

The size structure of the sampled population revealed three to four well-defined groups, each within a normal distribution, corresponding to distinct age classes. Both females and males were present in the smaller size ranges, but from 155 cm DW onwards, only females were observed. This pattern suggests that females reach larger sizes than males, a trend commonly seen in fishes, particularly among elasmobranchs (Pratt *et al.* 1990, Conrath and Musick 2012). Indeed, the largest individual recorded in this study was a female measuring 221.6 cm DW. The absence of large males may also suggest a slower growth rate or shorter lifespan in males than in females. Although some large individuals were occasionally observed, their representativeness may be underestimated, as some specimens were sectioned prior to being landed, making it difficult to account for them fully. The majority of the sampled individuals were immature. This could be due to two potential factors:

First, the fishing grounds off Salaverry may serve as a nursery area. Nursery or breeding grounds are generally found in shallow coastal waters. The continental shelf off La Libertad extends approximately 120 km, and the stretch between the La Libertad and Ancash regions comprises one of the most extensive continental shelves in the country (GEF *et al.* 2002, Graco *et al.* 2007, Martillo *et al.* 2011). Further studies, including those on other populations of *M. chilensis* along the Peruvian coast, would be needed to test this hypothesis. Such research could assess catch composition by size, ontogenetic variation (shifts in juvenile diet and habitat preferences), and the spatial distribution of mature females (Bejarano, 2007).

Second, the fishing nets do not discriminate between individuals based on their life stage. Local fishers use drift nets with a mesh size of 14–15 inches, smaller than the DW of the smallest specimen found (41 cm). This indicates that the gear does not discriminate by life stage and captures individuals of all sizes and cohorts indiscriminately. Prolonged fishing pressure on immature specimens could have serious long-term implications for the population, as it reduces the number of individuals that reach reproductive age, potentially leading to population decline (Oddone *et al.* 2008, Dulvy *et al.* 2014)

Seasonality is a consistent feature in most related studies, with the greatest abundance typically observed between August and November. A similar pattern was documented by Capapé *et al.* (2007) in *Myliobatis aquila*, with greater abundance noted from August to October (boreal summer to autumn), a period when temperatures resemble those of the sea off the coast of La Libertad during the austral spring (Observatoire National de la Mer et du Littoral 2016). In regions with minimal temperature variation throughout the year, abundance tends to remain constant, with slight increases in certain months: Villavicencio (1996) recorded greater numbers of *M. californica* specimens in May and June (boreal spring to summer), and *M. longirostris* from June to December. Notably, the temperatures in the sampling area are warm, averaging around 20°C (INAPESCA, 2013), which appear to be ideal conditions for *Myliobatis* species. In addition, prey availability plays a critical role, as high prey abundance typically correlates with increased predator populations. *M. chilensis* primarily feeds on Peruvian anchovy (*Engraulis ringens*) (Peña-Cutimbo *et al.* 2024), so fluctuations in anchovy availability are likely to influence its abundance. Consequently, during El Niño–Southern Oscillation (ENSO) events, vertical or latitudinal migrations of *M. chilensis* may occur in response to changes in water temperature and prey distribution.

4.2. Sex, weight–length ratio

Although specimens were randomly sampled, an overall sex ratio of 1:1 was observed, indicating that *M. chilensis* may exhibit a natural balance in the number of males and females. This equilibrium can enhance the reproductive potential of the species by maximizing mating opportunities for both sexes. Similar sex ratios have been documented in various elasmobranch species, including *Zapteryx xyster* from Santa Rosa, Ecuador (Vélez 2015), *Rhinobatos percellens* from Santa Marta, Colombia (Grijalba-Bendeck *et al.* 2012), and *Narcine entemedor* (Burgos-Vásquez *et al.* 2017) and *Rhinoptera steindacheri* from the southern Gulf of California (Burgos-Vásquez *et al.* 2018). These studies also reported seasonal trends in sex ratios, which align with those observed in the present study.

Immature rays are morphologically identical from adults. Growth curves were adjusted to a potential model, where both exponents (b) were equal to 3, indicating isometric growth (Cifuentes *et al.* 2012), suggesting that body proportions remain consistent as individuals increase in size: weight increases proportionally with length. A similar trend was observed in *Aetobatus narinari* from Venezuela, where the exponent (b) was 2.948 (Tagliafico 2012), and in a study from southern Africa, where the value was b=3.13 (Torres 1991). Torres (1991) also reported similar values for *Dasyatis pastinaca* (b=3.11) and *Gymnura natalensis* (b=3.02).

4.3. Biological indexes

Indexes are useful as an indirect method for estimating reproductive periods (Tresierra *et al.* 2002). An increase in GSI indicates periods when the ovaries are producing oocytes, while a decrease suggests that spawning has occurred (Tresierra *et al.* 2013). Peaks in HI reflect the liver's preparation

for reproduction, as it is the primary site of lipid storage and vitellogenin synthesis (Henningsen 1999). Conversely, decreasing HI values are associated with reproductive activity, reflecting energy expenditure during gamete production (Tresierra *et al.* 2013).

Because female gamete production requires greater energy investment, female livers were generally larger than those of males, even among individuals of similar body size. This sexual dimorphism in liver size is consistent with the energy demands of vitellogenesis. However, the variations in both HI and GSI did not exhibit clearly defined seasonal peaks, suggesting the absence of a distinct reproductive season in *M. chilensis*.

The relatively stable temperatures (Table S2 – Supplementary material) of the Humboldt Current throughout the year likely contribute to the species' continuous reproductive cycle. In contrast to other marine environments with strong seasonal shifts, the ecological niche of *M. chilensis* appears to lack extreme environmental fluctuations that would necessitate seasonally timed reproduction. This hypothesis is supported by anecdotal evidence from local fishers, who reported the presence of pregnant females year-round. However, these individuals often do not arrive at port intact, as they are typically cut into sections onboard for easier handling and storage, which may result in underrepresentation in landing records.

4.4. Reproductive system

The basic reproductive structure of *M. chilensis* is similar to that of other elasmobranchs, especially myliobatids. In the assessment of male maturity, the analysis of reproductive organs primarily served to corroborate findings based on the copulatory organs (Tresierra *et al.* 2002). External characteristics such as clasper size, rotation ability, rhipidion opening and calcification provided reliable, non-lethal indicators of maturity (Walker 2005). The development of copulatory structures is regulated by androgens; for instance, significant testosterone peaks have been recorded in *Mobula alfredi* during mating behaviour (Matsumoto *et al.* 2019), and clasper development in whale sharks has been associated with rising testosterone levels (Nozu *et al.* 2017). Thus, the degree of clasper development is considered a proxy for reproductive maturity.

In this study, linear regression demonstrated a strong correlation between gonad size and CL. However, as observed in *Rhinobatos steindachneri* (Burgos-Vásquez *et al.* 2018), some *M. chilensis* specimens exhibited well-developed testes but lacked full calcification of the claspers, and the apopyle and hypopyle remained closed. Although these individuals may be physiologically mature, their copulatory structures would not yet permit successful internal fertilization (Moya, 2017). Therefore, while gonadal development is essential for reproductive capability, functional maturity is best assessed through clasper morphology. Despite slight asymmetries in testis size, the presence of similar cysts in both organs suggests that both testes are functional.

Spermatogenesis in elasmobranchs is typically described in five phases (Tresierra *et al.* 2002, Acero *et al.* 2008, Moya 2017), though other classifications range from seven (Hoyos 2003, García 2018) to nine phases (Grijalba-Bendeck *et al.* 2008). Nevertheless, classification into 11 phases provides the most detailed characterization. Once mature, sperm is transported from the testes through the epididymis, often packaged into bundles during transit to prevent dispersion in seawater during ejaculation. Histological studies of the female's recipient organs and the epididymis of males would provide a more in-depth understanding of the reproductive system of *M. chilensis*.

In contrast to males, external morphological traits were insufficient for assessing reproductive maturity in females. Instead, histological and macroscopic analyses of the reproductive organs were required. The difference in size may be indicative of sexual dimorphism, and this could be complemented with an endocrine analysis (Nozu *et al.* 2015). Although ovarian size increased with DW, it was not a reliable indicator of maturity. For example, ovaries measuring 10–15 cm LO were observed in both immature and juvenile individuals. Therefore, morphological features offered more accurate maturity assessments.

Immature specimens showed an abundant epigonal organ, a haematopoietic organ responsible for blood supply and protection of developing structures. As individuals grow, the epigonal organ tends to shrink while gonads acquire greater vascularization and tissue thickening. In mature individuals, the right ovary remained largely undeveloped, still enveloped by the epigonal organ, whereas the functional LO showed clear signs of oogenesis. This unilateral development pattern is characteristic of several elasmobranchs, including *Carcharhinus falciformis* and *Sphyrna zygaena*, in which only the right ovary is functional (Hoyos 2003, Bejarano 2007). In some Myliobatiformes, such as *Rhinoptera steindacheri* (Burgos-Vásquez *et al.* 2018), *Gymnura marmorata* (Burgos-Vásquez *et al.* 2019), species of the genus *Mobula* (Serrano 2009) and *M. chilensis*, the LO is the only one capable of producing oocytes which are few but large. Smaller species may develop both functional ovaries, as seen in *Myliobatis aquila* (Capapé *et al.* 2007). The exclusive functionality of one ovary may reflect the high energetic costs of producing large oocytes.

Interestingly, no nidamental or oviducal gland was found in *M. chilensis*, a rare condition among elasmobranchs. This gland, typically responsible for sperm storage, fertilization and egg encapsulation, is usually reduced in viviparous and ovoviviparous species (Alva *et al.* 2012). Its complete absence, though previously reported in *Narcine entemedor* (Burgos-Vásquez *et al.* 2018), may represent an evolutionary adaptation in *M. chilensis*. Notably, the gland is still present in congeners such as *Myliobatis aquila* (Capapé *et al.* 2007), suggesting species-specific divergence.

The number of vitellogenic oocytes showed a positive correlation with both ovary and body size, but no relationship was found between body size and oocyte diameter. This may reflect asynchronous development, in which vitellogenic oocytes are released gradually rather than in a single spawning event. These oocytes are notably large and are protected by multiple surrounding cellular layers. After ovulation, they pass through the ostium into the oviduct, where fertilization occurs, and then migrate to the endometrium of the uterus.

The uteri are paired, with no apparent connection between the left and right sections. Colonello (2013) described asymmetry in the uteri of Myliobatiformes, noting that the left section is slightly larger than the right, although both are functional, as evidenced by the presence of developed trophonemata. Initially, uteri were not collected due to a lack of knowledge about the organ's appearance. Though we did not find embryos in formation, it was inferred that *M. chilensis* is viviparous, with histotrophic lipid nutrition. This conclusion was based on the presence of trophonemata in the larger uteri, which secreted a whitish substance known as "uterine milk" or histotroph. This secretion provides nutrition to the developing embryos, which grow relatively large. Although mature females were classified into a single stage, it is likely that histotrophic females with empty uteri were either ready to gestate or had miscarried during fishing operations. Smaller individuals found during fishing could potentially be neonates.

According to local fishers, pregnant females are present year-round, with more frequent captures between June and July. They also noted that pregnant females typically carried 2 to 6 embryos. These pups and embryos are locally known as *rayas mariposas* (butterfly rays) or simply *mariposas* (butterflies), though this term should not be confused with the common name of *Gymnura marmorata*, which was not reported in Salaverry. If accurate, this suggests that *M. chilensis* has slightly higher fecundity than other myliobatids: when the number of embryos in gestation was studied in two *Rhinoptera* species, both gestated a single embryo (Pérez-Jiménez 2011, Burgos-Vásquez *et al.* 2018).

Myliobatis is considered a relatively recent genus in the phylogeny of batoids (Dulvy and Reynolds 1997). Its large body size and K-selected life-history strategy—characterized by low fecundity, slow growth and late maturity—render it especially vulnerable to overfishing. This is exacerbated by its exposure to artisanal fisheries. The median size at sexual maturity was relatively high for both sexes, and the majority of specimens sampled were immature, indicating significant fishing pressure on non-reproductive individuals. Combined with increasing market demand and low reproductive output, these pressures could lead to population decline. To mitigate this, further studies are urgently needed to understand life-history traits, reproductive biology and population structure across the Humboldt

Current system. Management strategies such as seasonal closures, gear restrictions, marine protected areas and extraction quotas should be considered to ensure the long-term viability of *M. chilensis*.

Supplementary information ↑

Funding sources

This research was carried out to obtain a bachelor's degree and was self-financed. KK was supported by the Universidad Científica del Sur (RDN° 058-DGIDI-CIENTIFICA-2025).

Supplementary material

The supplementary material, which is available through the online version of this article, includes additional figures that document in detail the reproductive biology of *Myliobatis chilensis*. This material comprises macroscopic observations, histological sections, and morphometric relationships of both female and male reproductive systems, including oogenesis, spermatogenesis, and associated reproductive structures. The large number of supplementary figures reflects the comprehensive nature of the dataset, as this article is derived from the undergraduate thesis of the first author and aims to provide full methodological transparency and anatomical documentation supporting the main results.

Data availability

Not applicable.

Acknowledgements

We extend our sincere gratitude to medical technologist José Soldado Muro for his work in processing the histological samples. We also thank engineer Julio César Medina Lescano and biologist Santos Saenz Vásquez from the Ministry of Production for their valuable support. Special thanks are due to biologists Germán Vela Horna, Armando Isla Ventura, Betsy Buitrón Díaz and Ángel Perea De La Matta from the Peruvian Marine Institute (IMARPE) for their contributions. We are also grateful to the fishermen of the port of Salaverry for their collaboration during the sampling process. Finally, we thank the Universidad Científica del Sur for their assistance in reviewing the language of this publication.

Authorship contribution statement

MV-H and ZC conceived, designed the study. Conducted the investigation and formal analyses. MV-H led the methodology, project administration and preparation of the original draft. ZC and KK contributed to data analysis, review and editing of the manuscript. All authors reviewed and approved the final version of the manuscript.

Competing interests

The authors declare no competing interests.

Statement on the use of Artificial Intelligence

Artificial intelligence tools were occasionally used to assist with grammar, spelling, and syntax revision during manuscript preparation. The authors take full responsibility for the content of the manuscript.

REFERENCES

Acero P., Grijalba-Bendeck F., Moreno F., *et al.* 2008. Histología Comparada del Sistema Reproductivo de Cuatro Especies de Rayas Caribeñas (Chondrichthyes: Batoidea). Rev. Acad. Colom. Cienc. 32(125): 581-596. https://doi.org/10.18257/raccefyn.32(125).2008.2342

Alva R., Lujan L., Díaz M., *et al.* 2012. Ictiología. El Gráfico, Trujillo.

Bejarano O. 2007. Biología reproductiva del tiburón martillo *Sphyrna lewini* (Griffith y Smith, 1834) Salina Cruz, Oaxaca, México. Master's thesis, Instituto Politécnico, 93 pp.

Bradley R. 2012. Sudado de Raya: An Ancient Peruvian Dish. Gastronomica. 12: 68-73. https://doi.org/10.1525/GFC.2012.12.4.68

Burgos-Vázquez M.I., Mejía-Falla P., Cruz V., *et al.* 2017. Reproductive Strategy of the Giant Electric Ray in the Southern Gulf of California. Mar. Coast. Fish. 9: 577–596. https://doi.org/10.1080/19425120.2017.1370042

Burgos-Vásquez M.I., Chávez-García V.E., Cruz-Escalona V.H., *et al.* 2018. Reproductive strategy of the Pacific cownose ray *Rhinoptera steindachneri* in the southern Gulf of California. Marine and Freshwater Research. Mar. Freshw. Res. 70(1): 93-106. https://doi.org/10.1071/MF18096

Burgos-Vásquez M.I., Galván-Magaña F., Carrera Fernández M., *et al.* 2019. Reproductive characteristics and reproductive tract anatomy of the California butterfly ray *Gymnura marmorata* (Myliobatiformes: Gymnuridae). J. Fish Biol. 95(2): 490-501. https://doi.org/10.1111/jfb.13999

Capapé C., Guélorget O., Vergne Y., *et al.* 2007. Reproductive Biology of the Common Eagle Ray *Myliobatis aquila* (Chondrichthyes: Myliobatidae) from the Coast of Languedoc (Southern France, Northern Mediterranean). Vie et Milleu. 57(3): 125-130.

Cifuentes R., Gonzalez J., Montoya G., *et al.* 2012. Relación peso-longitud y factor de condición de los peces nativos del río San Pedro (cuenta del río Valdivia, Chile) Gayana. 75(2): 101-110. https://doi.org/10.4067/S0717-65382012000100009

Colonello J., Christiansen H., Macchi G. 2007. Escala de madurez sexual para peces cartilaginosos de la Plataforma Continental Argentina. INIDEP, Informe Técnico. 74: 1-15.

Colonello J., Christiansen H., Cousseau M., *et al.* 2013. Uterine dynamics of the Southern Eagle Ray *Myliobatis goodei* (Chondrichthyes: Myliobatidae) from the southwest Atlantic Ocean. Ital. J. Zool. 80: 187-194. https://doi.org/10.1080/11250003.2012.742146

Conrath C., Musick J. 2012. Reproductive Biology of Elasmobranchs. In: Carrier J.C., Musick J.A., Heithaus M.R. (eds), Biology of Sharks and Their Relatives. CBC Press, Boca Raton, pp. 291-306.

Dulvy N., Reynolds J. 1997. Evolutionary transitions among egg-laying, live-bearing and maternal inputs in sharks and rays. Proc. R. Soc. Lond. B Biol. Sci. 264: 1309-1315. https://doi.org/10.1098/rspb.1997.0181

Dulvy N.L, Fowler S.L., Musick J.A., *et al.* 2014. Extinction risk and conservation of the world's sharks and rays. E-Life. 3: e00590.

Dulvy N.K., Acuña E., Bustamante C., *et al.* 2020. *Myliobatis chilensis*. The IUCN Red List of Threatened Species 2020: e.T60123A124441181. https://doi.org/10.2305/IUCN.UK.2020-3.RLTS.T60123A124441181.en

Engel K.B., Callard G.V. 2005. The testis and spermatogenesis. In: Hamlett, W.C. (ed), Reproductive Biology and Phylogeny of Chondrichthyes. Science Publishers, New Hampshire, pp. 171-200

Ganias K., Kjesbu O., Lowerre-Barbieri S., *et al.* 2025. Reproduction of marine fishes. In: Cabral H., Lepage M., Lobry J. (eds), Ecology of Marine Fish. Academic Press, pp. 143-159. https://doi.org/10.1016/B978-0-323-99036-3.00017-9

García G. 2018. Biología reproductiva del tiburón *Mustelus lunulatus* (Jordan y Gilbert 1883) en Bahía Tortugas, Baja California Sur, México. PhD thesis, Instituto Politécnico Nacional, 114 pp. http://repositoriodigital.ipn.mx/handle/123456789/26215

GEF, ONUDI, IMARPE and FOP. 2002. Proyecto Manejo Integrado Gran Ecosistema Marino de la Corriente de Humboldt Módulo I: Productividad. 49 pp. http://humboldt.iwlearn.org/es/informacion-y-publicacion/GEFMODULOIProductividadVol1.pdf

Gilbert P.W., Heath G.W. 1972. The clasper-siphon sac mechanism in *Squalus acanthias* and *Mustelus canis*. Comp. Biochem. Physiol. 42: 97–119. https://doi.org/10.1016/0300-9629(72)90371-4

González-Pestana A., Mangel J.C., Alfaro-Córdova E., *et al.* 2020. Diet, trophic interactions and possible ecological role of commercial sharks and batoids in northern Peruvian waters. J. Fish Biol. 98(3): 768-783. https://doi.org/10.1111/jfb.14624

González-Pestana A., Velez-Zuazo X., Alfaro Shigueto J., *et al.* 2023. Batoid fishery in Peru (1950-2015): Magnitude, management and data needs. Rev. Biol. Mar. Oceanogr. 57: 217-233. https://doi.org/10.22370/rbmo.2022.57.Especial.3729

Graco M., Ledesma J., Flores G. *et al.* 2007. Nutrientes, oxígeno y procesos biogeoquímicos en el sistema de surgencias de la corriente de Humboldt frente a Perú. Rev. peru biol. 14(1): 117-128. https://doi.org/10.15381/rpb.v14i1.2165

Grijalba–Bendeck M., Acero A., González E. 2008. Biología reproductiva de *Rhinobatos percellens* (Walbaum, 1792) (Batoidea: Rajiformes) en el Caribe colombiano. Rev. Biol. Mar. Oceanogr. 43(3): 469–481. https://doi.org/10.4067/S0718-19572008000300006

Grijalba–Bendeck M., Polo-Silva C., Acevedo K., *et al.* 2012. Aspectos tróficos y reproductivos de algunos batoideos capturados en Santa Marta, Mar Caribe de Colombia. Lat. Am. J. Aquat. Res. 40(2): 300–315. https://doi.org/10.3856/vol40-issue2-fulltext-6

Grupo de Trabajo Institucional El Niño. 2017. Informe de las Condiciones Oceanográficas y Biológico Pesqueras Octubre del 2017. Boletín informativo IMARPE. http://www.imarpe.pe/imarpe/archivos/informes/imarpe_atsm_gti_mens_octubre2017.pdf

Henningsen A. 1999. Levels of recirculating reproductively-related steroid hormones in female elasmobranchs. Implications for reproduction in a captive environment. Aquarium Sciences and Conservation. 2: 97-116. https://doi.org/10.1023/A:1009688826898

Hoyos E. 2003. Biología Reproductiva del Tiburón Piloto *Carcharhinus falciformis* (BIBRON, 1839) de Baja California Sur. Master's thesis, Instituto Politécnico Nacional, 75 pp. https://tesis.ipn.mx/bitstream/handle/123456789/3293/49.pdf?sequence=1&isAllowed=y

INAPESCA. 2013. Boletín hidrometerológico noviembre 2013.

Martillo C., Pazmiño A., Chunga K., *et al.* 2011. Descripción Morfológica de la Plataforma Continental del Ecuador y Análisis Comparativo con la Plataforma Jurídica Mediante la Aplicación de Sistemas de Información Geográfica. Acta Oceanográfica del Pacífico. 16(1): 109-118.

Matsumoto R., Matsumoto Y., Ueda K., *et al.* 2019. Sexual maturation in a male whale shark (*Rhincodon typus*) based on observations made over 20 years of captivity. Fish. Bull. 117(1-2): 78-86. https://doi.org/10.7755/FB.117.1-2.9

Moya A.C. 2017. Biología reproductiva de dos especies de rayas del golfo San Matías: la raya platana *Atlantoraja platana* y la raya marmorada *Sympterygia bonapartii*. Un enfoque morfofuncional. PhD thesis, Universidad Nacional del Sur, 250 pp.

Nozu R., Murakumo K., Matsumoto R., *et al.* 2015. Gonadal Morphology, Histology, and Endocrinological Characteristics of Immature Female Whale Sharks, *Rhincodon typus*. Zoolog. Sci. 32(5): 455–458. https://doi.org/10.2108/zs150040

Nozu R., Murakumo K., Matsumoto R., *et al.* 2017. High-resolution monitoring from birth to sexual maturity of a male reef manta ray, *Mobula alfredi*, held in captivity for 7 years: changes in external morphology, behavior, and steroid hormone levels. BMC Zool. 2: 14. https://doi.org/10.1186/s40850-017-0023-0

Nureña M.S. 2018. Biología reproductiva de *Ethmidium maculatum* "machete" (Valenciennes, 1847) proveniente de la región La Libertad, de mayo 2017 a abril 2018. Bachelor's thesis, Universidad Nacional de Trujillo, 70 pp. https://repositorio.imarpe.gob.pe/bitstream/20.500.12958/3253/1/Nure%c3%b1a%20Mu%c3%b1oz.pdf

Observatoire National de la Mer et du Littoral. 2016. Variabilité de la Température et de la Salinité dans les Eaux Métropolitaines. Downloaded on 20 December 2018: http://www.onml.fr/onml_f/fiches/Variabilite_de_la_temperature_et_de_la_Salinite_dans_les_eaux_metropolitaines/temperature-salinite.pdf

Oddone M., Amorim A., Mancini P. 2008. Reproductive biology of the spotback skate, *Atlantoraja castelnaui* (Ribeiro, 1907) (Chondrichthyes, Rajidae), in southeastern Brazilian waters. Rev. Biol. Mar. Oceanogr. 43(2): 327-334. https://doi.org/10.4067/S0718-19572008000200010

Peña-Cutimbo N., Córdova-Zavaleta F., Velarde-Vílchez M., *et al.* 2024. Comparative feeding analysis between the Chilean eagle ray *Myliobatis chilensis* (Philippi, 1982) and the Peruvian eagle ray *Myliobatis peruvianus* (Garman, 1913) from northern Peru. Reg. Stud. Mar. Sci. 81: 1-10. https://doi.org/10.2139/ssrn.4863015

Pérez-Jiménez J.C. 2011. Biología reproductiva de la raya *Rhinoptera bonasus* (Elasmobranchii) en el sureste del Golfo de México. Hidrobiológica. 21(2): 159-167.

Pratt H.L. 1988. Elasmobranch gonad structure: A description and survey. Copeia, 3: 719–729. https://doi.org/10.2307/1445394

Pratt H.L., Gruber S., Taniuchi T. 1990. Elasmobranchs as living resources: advances in the biology, ecology, systematics, and the status of the fisheries. NOAA Technical Report NMFS, 528 pp. https://spo.nmfs.noaa.gov/sites/default/files/tr90opt.pdf

PRODUCE. 2018. Anuario estadístico pesquero y acuícola 2018. Ministerio de la Producción, Lima, 200 pp.

Sáez S., Lamilla J. 2012. Claves taxonómicas para el reconocimiento dentario en taxa del superorden Rajomorphii de Chile (Chondrichthyes, Batoidea). Lat. Am. J. Aquat. Res. 40: 282-291. https://doi.org/10.3856/vol40-issue2-fulltext-4

Serrano J. 2009. Estudio Comparativo de la Reproducción de Tres Especies del Género *Mobula* (Chondrichthyes: Mobulidae) en el suroeste del Golfo de California, México. PhD thesis, Instituto Politécnico Nacional, 86 pp. https://www.repositoriodigital.ipn.mx/bitstream/123456789/14110/1/serranol1.pdf

Torres F.S.B. 1991. Tabular data on marine fishes from Southern Africa, Part I. Length-weight relationships. Fishbyte. 9: 50–53.

Tresierra A., Culquichicón Z., Veneros B. 2002. Biología Reproductiva en Peces. CONCYTEC, Trujillo, 286 pp.

Tresierra A., Culquichicón Z., Solano A. 2013. Métodos para la Gestión de los Recursos Pesqueros. CONCYTEC, Trujillo, 350 pp.

Tresierra A., Culquichicón Z., Veneros B. 2014. Manual de Evaluación de Recursos Pesqueros. CONCYTEC, Trujillo.

Tagliafico, A. 2012. Exploitation and reproduction of the spotted Eagle ray (*Aetobatus narinari*) in the Los Frailes Archipelago, Venezuela. Fish. Bull. 110: 307-316

Vélez J. 2015. Aspectos Reproductivos de la raya ocelada *Zapteryx xyster* (Jordan & Evermann, 1896) en Santa Rosa, Salinas, Ecuador. PhD thesis, Universidad Laica "Eloy Alfaro" de Manabí, 107 pp. https://repositorio.uleam.edu.ec/bitstream/123456789/531/1/ULEAM-BLGO-0001.pdf

Veneros B., Amaya P.A. 2021. Characterization of the Artisanal Fishery of Elasmobranchs in Puerto Casma, Ancash, Peru: 2010-2015. Ann. Rom. Soc. Cell. Biol. 25(7): 1305-1313.

Villavicencio C. 1996. Tallas, proporción de sexos y reproducción de *Myliobatis californica* y *M. longirostris* (Pisces: Myliobatidae) en Baja California Sur, México. Rev. Biol. Trop. 43(2): 291-295.

Walker T.I. 2005. Reproduction in Fisheries Science. In: Hamlett W.C (ed), Reproductive Biology and Phylogeny of Chondrichthyes: Sharks, Batoids and Chimaeras. Science Publishers, Enfield, pp. 45-79.

Zavalaga F., Campos León S., Kanagusuku K. 2021. Principales Rayas del Perú. Instituto del Mar del Perú, 96 pp.